Author Manuscript

Author Manuscript

Author Manuscript

Author Manuscript

HHS Public Access

Author manuscript

Cell Rep. Author manuscript; available in PMC 2016 February 17.

Published in final edited form as:

Cell Rep. 2015 October 6; 13(1): 209–221. doi:10.1016/j.celrep.2015.08.069.

LncRNA *HOTAIR* Enhances the Androgen-Receptor-Mediated Transcriptional Program and Drives Castration-Resistant Prostate Cancer

Ali Zhang[1,5], **Jonathan C. Zhao**[1,5], **Jung Kim**[1], **Ka-wing Fong**[1], **Yeqing Angela Yang**[1], **Debabrata Chakravarti**[2,4], **Yin-Yuan Mo**[3], and **Jindan Yu**[1,4,*]

[1]Division of Hematology/Oncology, Department of Medicine, Feinberg School of Medicine, Northwestern University, Chicago, IL 60611, USA

[2]Division of Reproductive Science in Medicine, Department of Obstetrics and Gynecology, Feinberg School of Medicine, Northwestern University, Chicago, IL 60611, USA

[3]Department of Pharmacology/Toxicology and Cancer Institute, University of Mississippi Medical Center, Jackson, MS 39216, USA

[4]Robert H. Lurie Comprehensive Cancer Center, Northwestern University Feinberg School of Medicine, Chicago, IL 60611, USA

SUMMARY

Understanding the mechanisms of androgen receptor (AR) activation in the milieu of low androgen is critical to effective treatment of castration-resistant prostate cancer (CRPC). Here, we report *HOTAIR* as an androgen-repressed lncRNA, and, as such, it is markedly upregulated following androgen deprivation therapies and in CRPC. We further demonstrate a distinct mode of lncRNA-mediated gene regulation, wherein *HOTAIR* binds to the AR protein to block its interaction with the E3 ubiquitin ligase MDM2, thereby preventing AR ubiquitination and protein degradation. Consequently, *HOTAIR* expression is sufficient to induce androgen-independent AR activation and drive the AR-mediated transcriptional program in the absence of androgen. Functionally, *HOTAIR* overexpression increases, whereas *HOTAIR* knockdown decreases, prostate cancer cell growth and invasion. Taken together, our results provide compelling evidence of lncRNAs as drivers of androgen-independent AR activity and CRPC progression, and they support the potential of lncRNAs as therapeutic targets.

This is an open access article under the CC BY-NC-ND license (http://creativecommons.org/licenses/by-nc-nd/4.0/).

*Correspondence: jindan-yu@northwestern.edu.

[5]Co-first author

ACCESSION NUMBERS

The accession number for the microarray and short-read sequencing data reported in this paper is GEO: GSE61270.

SUPPLEMENTAL INFORMATION

Supplemental Information includes Supplemental Experimental Procedures, five figures, and four tables and can be found with this article online at http://dx.doi.org/10.1016/j.celrep.2015.08.069.

AUTHOR CONTRIBUTIONS

A.Z., J.K., K.F., and Y.A.Y performed the experiments. J.C.Z. analyzed microarray and ChIP-seq data. J.Y. and A.Z. wrote the manuscript. D.C. provided critical discussions and Y.Y.M. helped with RIP and RNA pull-down protocols. J.Y. designed and supervised the project. All authors discussed the results and commented on the manuscript.

Author Manuscript Author Manuscript Author Manuscript Author Manuscript

Graphical abstract

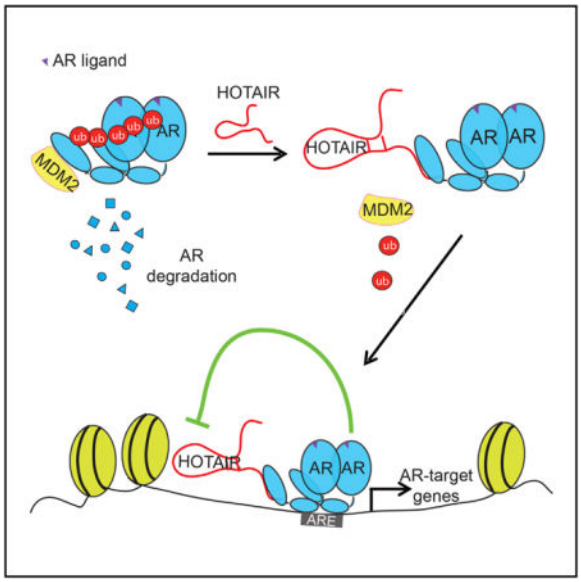

INTRODUCTION

Long noncoding RNAs (lncRNAs) are RNA transcripts that are more than 200 nt long but have little protein-coding potential. Within the last few years, thousands of lncRNAs have been identified and their function in biological processes begun to be understood (Iyer et al., 2015; Rinn and Chang, 2012). For example, lncRNA-*p21* has been shown to act in *trans* or in *cis* to regulate target gene expression (Dimitrova et al., 2014). LncRNAs also regulate chromatin states by association with chromatin-modifying proteins, such as the polycomb repressive complexes (PRC2) (Gupta et al., 2010a; Khalil et al., 2009). The lncRNA *HOTAIR* has been shown to bind PRC2 through its 5′ region but to bind the LSD1/REST complex with its 3′ domain, thereby serving as scaffolds that coordinate co-targeting of these proteins to selected chromatin regions (Tsai et al., 2010). In addition, emerging evidence suggests that lncRNAs are able to regulate cellular processes through post-translational mechanisms. For instance, lncRNA *FAL1* associates with BMI to regulate its stability and target gene transcription (Hu et al., 2014), whereas lncRNA *HOTAIR* interacts with E3 ubiquitin ligases through their RNA-binding domains to accelerate substrate ubiquitination and protein degradation (Yoon et al., 2013). Through these regulatory mechanisms, lncRNAs are believed to play critical roles in human development and diseases.

Prostate cancer (PCa) is a frequently diagnosed disease in American men. Androgen ablation therapies (ADTs) are the mainline treatment for patients with advanced PCa. Despite the high initial response rates, remissions following ADT are temporary due to the emergence of castration-resistant prostate cancer (CRPC). Studies of CRPC have revealed that resumption of androgen receptor (AR)-dependent transcriptional activity is a critical event in nearly all cases (Grasso et al., 2012). Identifying new molecular mechanisms underlying aberrant AR activation in the milieu of low androgen holds great promise to

Author Manuscript Author Manuscript Author Manuscript Author Manuscript

improve the treatment of CRPC. Integrative genomic analysis of microarray datasets has revealed many lncRNAs that were dys-regulated in various cancer types when compared to corresponding benign samples (Du et al., 2013). Transcriptome sequencing across PCa cohorts has identified a list of lncRNAs that stratify benign, localized, and metastatic PCa samples (Iyer et al., 2015; Prensner et al., 2011). These cancer-expressed lncRNAs, like protein-coding genes, may serve as markers of the disease and may play essential roles in cancer progression. In particular, *SChLAP1*, an lncRNA that is overexpressed in a subset of PCa, has been shown to promote PCa invasiveness and tumor metastasis by antagonizing the tumor-suppressive SWI/SNF chromatin-modifying complex (Prensner et al., 2013). Yang et al. (2013) reported two lncRNAs, *PRNCR1* and *PCGEM1*, that are highly overexpressed in aggressive PCa and bind successively to the AR protein to enhance the AR-mediated gene activation program and induce PCa growth. Yet, a subsequent study reported conflicting results (Prensner et al., 2014). Thus, lncRNAs that interfere with the critical AR pathway remain to be characterized.

HOTAIR, a 2.2-kb-long transcript localized to the boundaries of the *HOXC* gene cluster, is highly expressed and correlated with metastasis in a variety of cancer types, including breast (Gupta et al., 2010a; Sørensen et al., 2013), colorectal (Kogo et al., 2011), lung (Nakagawa et al., 2013), and pancreatic (Kim et al., 2013) cancers. *HOTAIR* promotes breast cancer metastasis at least in part by associating with the PRC2 complex to induce genome-wide retargeting of PRC2 to hundreds of genes involved in tumor metastasis (Gupta et al., 2010a). Integrative genomic analyses have revealed *HOTAIR* among hundreds of lncRNAs that are deregulated in various cancers (Du et al., 2013). *HOTAIR*, however, has not been well characterized in PCa. Through lncRNA profiling, a recent study showed that *HOTAIR* was inhibited by genistein, a phytoestrogen, and may have tumor-suppressive roles (Chiyomaru et al., 2013). This study, however, was carried out solely in the AR-negative DU145 and PC3 cell lines that do not represent clinical CRPC. In our study, we investigated whether the lncRNA *HOTAIR* interacts with the AR protein, modulates the AR-mediated transcriptional program, and contributes to CRPC.

RESULTS

HOTAIR Is Repressed by Androgen and Upregulated in CRPC

To identify lncRNAs that are potentially regulated by AR, we re-analyzed chromatin immunoprecipitation sequencing (ChIP-seq) data that we previously published in lymph node carcinoma of prostate (LNCaP) cells (Yu et al., 2010). Of 8,403 lncRNAs annotated in Ensemble, 3,418 contained at least one AR-binding event within 50 kb upstream of intragenic regions (Figure 1A; Table S1). Among these, we nominated *HOTAIR*, an lncRNA that has been studied in multiple cancer types, but has not been well characterized in PCa, for further investigation. ChIP-seq showed three strong AR-binding events at 46 kb upstream and 66 and 137 kb downstream of the *HOTAIR* gene (Figure S1A). As AR is known to regulate target genes through strong binding to enhancers and weak binding at promoters mediated by chromatin looping, we asked whether AR binds to the *HOTAIR* promoter. Motif analysis of the *HOTAIR* promoter revealed three highly scored androgen response element (ARE) motifs (Figure S1B). We then designed three primer pairs flanking

Author Manuscript Author Manuscript Author Manuscript Author Manuscript

these three AREs as well as a primer set targeting a distal region as a negative control. ChIP-PCR confirmed strong enrichment of known AR target enhancers of *PSA*, *TMPRSS2*, *FKBP5*, as well as the *HOTAIR* promoter, but not the distal region, by AR antibody relative to the IgG control (Figure 1B). Moreover, ChIP-qPCR in LNCaP cells demonstrated that androgen greatly increased AR binding to the *HOTAIR* promoter as well as known AR target enhancers, but not to the distal *HOTAIR* region (Figure S1C).

Next, we asked whether AR binding at *HOTAIR* regulatory regions results in modulation of gene expression. Our qRT-PCR analysis of LNCaP cells stimulated with R1881 showed that *HOTAIR* expression is highly sensitive to androgen; *HOTAIR* was inhibited by androgen rapidly and significantly up to 10-fold, while PSA showed a 14-fold increase (Figures 1C, 1D, and S1D). A similar decrease in *HOTAIR* expression following androgen treatment also was observed in another independent PCa cell line, vertebral cancer of prostate (VCaP) (Figures S1E and S1F). To demonstrate that this regulation is mediated by AR, we carried out AR knockdown through RNA interference and found that *HOTAIR* expression is markedly restored in AR-depleted LNCaP cells (Figures 1E and 1F). To further support that androgen inhibits *HOTAIR* through modulation of active transcription, we performed RNA PolII ChIP-qPCR and indeed observed a decrease in RNA PolII occupancy at *HOTAIR* and several known AR-repressed genes, but an increase at AR-induced genes such as *PSA* and *KLK2* (Figure S1G). Concordantly, ChIP-seq revealed slightly decreased enhancer activity (indicated by H3K27Ac) around the *HOTAIR* gene upon androgen stimulation (Figure S1A). By contrast, RNA decay assays showed no significant difference in the rates of *HOTAIR* lncRNA degradation in ethanol- and androgen-treated cells, precluding RNA stability as a mechanism to *HOTAIR* repression by androgen (Figure S1H).

Due to its androgen-regulated nature, we hypothesized that *HOTAIR* may be differentially expressed during PCa progression. We performed qRT-PCR analysis of a panel of PCa cell lines and observed that *HOTAIR* was drastically upregulated in CRPC cell line models, such as LNCaP-abl and C4-2B (Figure S1I). To confirm this in primary specimens, we re-analyzed two publicly available datasets and found that *HOTAIR* was significantly upregulated in metastatic CRPC when compared to localized prostate tumors (Figures 1G and 1H). Next, we stratified localized PCa into two groups based on biochemical recurrence and found that *HOTAIR* was significantly upregulated in patients with recurrent PCa (Figure 1I). Further, Kaplan-Meier analysis revealed that high *HOTAIR* level was significantly associated with poor clinical outcome (Figure 1J). To further validate these findings in independent patient cohorts, we conducted RNA in situ hybridization (ISH) in PCa tissue microarray (Figure 1K). Our data demonstrated that *HOTAIR* staining was indeed significantly stronger in recurrent PCa compared to non-recurrent PCa (Figure 1L). Therefore, *HOTAIR* is an androgen-repressed lncRNA and is upregulated in aggressive PCa and in CRPC tumors.

The lncRNA *HOTAIR* Directly Interacts with the AR Protein

Since both *HOTAIR* and AR are upregulated in late-stage PCa, we sought to determine whether *HOTAIR* might interact with AR protein. We performed in vitro transcription to synthesize biotinylated RNA from sense and antisense *HOTAIR* 1–360 bp, the region that

Author Manuscript Author Manuscript Author Manuscript Author Manuscript

interacts with EZH2, which was then incubated with nuclear extracts from LNCaP cells to allow protein interactions, precipitated using streptavidin beads, and analyzed by SDS-PAGE gel. Silver staining revealed that *HOTAIR*, but not the antisense fragment, precipitated a protein of 110 kDa (Figure S2A). To investigate whether this band represents the AR protein, we carried out western blot analysis and demonstrated that biotinylated *HOTAIR* RNA, but not the antisense transcript or no-probe control, retrieved AR protein (Figure 2A).

To further validate this interaction between *HOTAIR* and AR, we carried out RNA immunoprecipitation (RIP) of LNCaP cell nuclear extracts. A qPCR analysis of antibody-enriched RNA revealed that AR antibody (PG-21 targeting the N terminus of AR, EMD Millipore) pulled down significantly more *HOTAIR* lncRNA than the IgG control (Figure 2B). By contrast, no differential enrichment of U1 RNA was observed. This was validated using a second AR antibody targeting the C terminus of AR (C-19, SC-815x from Santa Cruz Biotechnology) (Figure S2B). In addition, RIP experiments showed that AR antibodies were able to significantly enrich *HOTAIR* in hormone-deprived cells, albeit with slightly reduced fold enrichment (Figures S2C and S2D). The amount of *HOTAIR* immunoprecipitated by the anti-AR antibodies was comparable to that enriched by EZH2 antibody, supporting a strong interaction between *HOTAIR* transcript and the AR protein (Figure S2E). Moreover, RIP analysis of C4-2B cell lysate confirmed such interaction and further showed that more *HOTAIR* transcript was enriched by anti-AR antibody in C4-2B than in LNCaP cells, supporting increased *HOTAIR* expression and regulatory activities in CRPC cells (Figure 2C).

Next, we sought to determine which region of the *HOTAIR* transcript mediates its interaction with the AR protein. We generated a series of *HOTAIR* deletion probes, which were biotinylated and utilized for RNA pull-down assay. We first confirmed that all of these probes were able to retrieve the *HOTAIR* gene itself with RNA pull-down efficiency around 15-fold when compared with the antisense control (Figure S2F). Next, RNA pull-down followed by western blot analysis showed that RNA probes containing 1–360 nt of the *HOTAIR* gene, but not others, were capable of pulling down AR, suggesting that the first 360 bp of *HOTAIR* are necessary and sufficient to bind the AR protein (Figure 2D). As a positive control, the 5′ end of *HOTAIR* also pulled down the EZH2 protein as previously reported (Tsai et al., 2010). On the other hand, we were interested in knowing which AR domain modulates its interaction with *HOTAIR*. To test this, we generated a series of FLAG-tagged AR domain constructs, which were subsequently transfected into 293T cells (Figure S2G). RNA pull-down experiments revealed that AR constructs containing the N-terminal domain (NTD), but not the DNA-binding domain (DBD) and ligand-binding domain (LBD), interact with *HOTAIR* (Figure 2E). To further demonstrate that this is a direct interaction, we synthesized the AR-NTD protein through in vitro translation (Figure 2F). In vitro binding assay that incubates AR-NTD with increasing amounts of *HOTAIR* 1–360-bp probes showed that *HOTAIR* sense probe pulled down the AR protein in a dose-dependent manner, whereas the antisense probe did not (Figure 2G). To determine whether this interaction crosstalks with the well-known AR protein interaction with DNA through its DBD, we performed electrophoretic mobility shift assay (EMSA) and found that *HOTAIR* probe, and

Author Manuscript Author Manuscript Author Manuscript Author Manuscript

thus its interaction with AR-NTD, did not disrupt the interaction between AR-DBD and biotinylated ARE, whereas ARE oligo fully blocked the gel shift as expected (Figure S2H). Therefore, our data strongly suggest that the NTD of the AR protein directly interacts with the 5′ end of the *HOTAIR* lncRNA.

HOTAIR Stabilizes AR Protein by Blocking Its Interaction with MDM2

To investigate the consequences of *HOTAIR* and AR interaction, we overexpressed *HOTAIR* in LNCaP and LAPC4 cells through lentivirual transduction followed by antibiotic selection of stable clones (Figure S3A). Immunoblotting analysis showed that AR protein level increased following *HOTAIR* overexpression in both cell lines (Figure 3A). However, qRT-PCR analysis revealed a lack of change of *AR* at the mRNA level (Figure S3B). Since *HOTAIR* lncRNA previously has been shown to interact with nuclear proteins, we performed nuclear and cytoplasmic extraction of LNCaP and LAPC4 cell lysates and confirmed that AR primarily localized in the nuclei, which is significantly increased by *HOTAIR* overexpression (Figures 3B and S3C). To test whether *HOTAIR* stabilizes AR protein, we treated LNCaP and LAPC4 cells with cycloheximide (CHX), an inhibitor of protein biosynthesis. Western blot analysis showed that the half-life of AR protein was about 4 hr in control cells, which was increased to about 16 hr in both LNCaP and LAPC4 cells with *HOTAIR* overexpression (Figures 3C and S3D). On the other hand, *HOTAIR* knockdown dramatically accelerated AR protein degradation in C4-2B cells, which could be rescued by concurrent overexpression of small hairpin RNA (shRNA)-resistant *HOTAIR* (Figure S3E). To further demonstrate that *HOTAIR* hinders AR protein degradation, we treated control and *HOTAIR*-overexpressing LNCaP cells with proteasome inhibitor MG132. Western blot analysis confirmed that MG132 dramatically increased AR protein level, confirming successful blockade of proteasome-mediated protein degradation (Figure 3D). Further, while *HOTAIR* overexpression significantly increased AR protein level in the control-treated cells, it had a much smaller effect on the cells pretreated with MG132, supporting a mechanism dependent on proteasome-mediated AR degradation.

AR previously has been shown to degrade through the ubiquitination pathway (Lin et al., 2002). To examine whether *HOTAIR* affects AR ubiquitination, we performed co-transfection of FLAG-AR, HA-ubiquitin, *HOTAIR* or various *HOTAIR* deletion constructs into 293T cells. Western blot analysis of whole-cell lysate (WCL) confirmed AR protein expression in all experimental conditions. Cell lysates were then subjected to immunoprecipitation (IP) by an anti-HA antibody followed by western blotting using an anti-AR antibody. Our results showed that the presence of ubiquitin led to AR protein ubiquitination, which was blocked by the co-expression of *HOTAIR* that contained the first 360 bp, but not others (Figure 3E). Concordantly, reverse coIP using an anti-FLAG (AR) antibody followed by western blotting using an anti-ubiquitin antibody confirmed that *HOTAIR* transcripts prevent AR from binding to ubiquitin proteins (Figure 3F).

Previous studies have shown that MDM2, an E3 ligase, interacts with AR through its NTD domain, leading to AR protein ubiquitination (Lin et al., 2002). We thus hypothesized that *HOTAIR* binding with the AR protein masks the NTD and, thus, prevents AR from interacting with MDM2. To test this, we co-transfected 293T cells with AR, FLAG-tagged

Author Manuscript Author Manuscript Author Manuscript Author Manuscript

MDM2, and increasing doses of *HOTAIR*. Western blot analysis of WCL confirmed AR and FLAG (MDM2) expression. FLAG IP followed by western blot of AR proteins demonstrated that MDM2 physically interacts with the AR protein, which, however, is inhibited by concomitant *HOTAIR* expression in a dose-dependent manner (Figure 3G). To confirm this mechanism in a physiological setting, we performed IP using an anti-AR antibody in LNCaP cells with control and *HOTAIR* overexpression and in C4-2B cells with control and *HOTAIR* knockdown. Immunoblotting using an anti-MDM2 antibody demonstrated decreased and increased MDM2 pull-down, respectively, following *HOTAIR* overexpression in LNCaP cells and *HOTAIR* knockdown in C4-2B cells (Figure S3F). Taken together, our data suggest that *HOTAIR* stabilizes AR protein by binding to its NTD, thus blocking MDM2-AR interaction and decreasing AR ubiquitination and protein degradation.

HOTAIR Expression Enhances AR Transcriptional Activity

Next, to determine how *HOTAIR* affects the genomic action of AR, we first extracted nuclear and chromatin-bound protein fractions. Western blot analysis showed that *HOTAIR* expression dramatically increased both nuclear and chromatin-bound AR protein (Figure 4A). To examine whether this leads to an increase in AR-binding events, we performed AR ChIP-seq in LNCaP cells with either control or *HOTAIR* overexpression. Remarkably, ChIP-seq analysis revealed that the amount of AR-binding events was nearly doubled in LNCaP cells with *HOTAIR* overexpression (Figure 4B). In contrast to the marked gain of new AR-binding sites (ARBSs), very few were lost probably due to variability between replicate experiments. Moreover, all ARBSs, including gained, lost, and conserved ones, showed increased enrichment following *HOTAIR* overexpression (Figure 4C). A genome browser view of several known AR-bound enhancers confirmed highly enriched and sharp AR-binding peaks at target sites in *HOTAIR*-overexpressing cells (Figures 4D, 4E, S4A, and S4B).

To validate these findings, we performed AR ChIP-qPCR on several known AR target genes using site-specific primers. Our data confirmed that *HOTAIR* overexpression indeed increased AR recruitment to enhancers of *PSA*, *TMPRSS2*, *FKBP5*, *OPRK1*, and *MET* (Zhao et al., 2012; Figure 4F). Consistent with this increase in AR occupancy, qRT-PCR demonstrated that *HOTAIR* increased the expression of AR-induced genes, whereas it reduced that of AR-repressed genes in both LNCaP and LAPC4 cells, supporting overall augmentation of AR transcriptional activity (Figures 4G and S4C). Further, *HOTAIR*-induced AR target gene expression was fully abolished by AR knockdown via RNA interference (Figure 4H). Together, these results suggest that *HOTAIR* enhances AR chromatin-binding and transcriptional activity.

HOTAIR Drives Androgen-Independent AR Chromatin Targeting

We sought to determine whether *HOTAIR* overexpression is able to activate AR even in the absence of androgen. Western blot analysis showed a dramatically increased amount of nuclear AR in *HOTAIR*-expressing, but hormone-deprived, LNCaP cells (Figure 5A). Concordantly, AR immunofluorescence staining in hormone-deprived or -stimulated control and *HOTAIR*-expressing LNCaP cells revealed that, similar to androgen stimulation,

Author Manuscript Author Manuscript Author Manuscript Author Manuscript

HOTAIR overexpression resulted in evident AR nuclear staining in the absence of androgen (Figure 5B). ChIP-seq showed that, as expected, very few ARBSs were detected in the control, hormone-deprived cells. Remarkably, *HOTAIR* overexpression increased AR-binding events from 112 to 5,566 sites, strongly supporting androgen-independent AR activation (Figures 5C and 5D). A genome browser view confirmed that *HOTAIR* overexpression resulted in substantial AR-binding events at the enhancers of known AR target genes, such as *TMPRSS2*, *FKBP5*, *PSA*, and *KLK2* (Figures 5E, 5F, S5A, and S5B). Moreover, ChIP-qPCR confirmed that *HOTAIR* overexpression is sufficient to dramatically induce AR binding to target genes even under androgen-depleted conditions (Figure 5G).

Next, we asked whether *HOTAIR* expression is required for AR transcriptional activity in CRPC cells. Since we have shown that *HOTAIR* is upregulated in CRPC cell lines, we carried out *HOTAIR* knockdown in C4-2B cells (Figure S5C). ChIP-seq showed that, unlike the androgen-dependent LNCaP cells, C4-2B cells harbor substantial AR-binding events even in the absence of androgen, being consistent with androgen-independent AR activation (Figure 5H). Most importantly, *HOTAIR* knockdown abolished a majority of these AR-binding events, suggesting that *HOTAIR* is required for androgen-independent AR activation in CRPC cells. Analysis of ChIP-seq read counts around these ARBSs confirmed a significant decrease at most ARBSs (Figure 5I). Further, ChIP-qPCR verified that *HOTAIR* knockdown in C4-2B cells decreased AR binding at known AR target genes, which could be rescued by the overexpression of shRNA-resistant *HOTAIR* gene (Figure 5J). Taken together, our results support that *HOTAIR* expression is critical in inducing and maintaining androgen-independent AR activation and genomic targeting.

HOTAIR Induces AR Transcriptional Program in the Absence of Androgen

To understand how the *HOTAIR*-mediated AR program relates to that induced by androgen, we first compared the ARBSs induced by *HOTAIR* (under androgen-deprived conditions) with those by androgen in LNCaP cells. Interestingly, we found that more than 70% of *HOTAIR*-induced ARBSs overlapped with androgen-induced ones, supporting that, instead of reprogramming AR, *HOTAIR* primarily acts to increase AR activity (Figure 6A). A heatmap view of AR ChIP-seq reads around all ARBSs further confirmed that, under androgen-deprived conditions, *HOTAIR* overexpression induced an AR-binding profile that highly resembles that stimulated by androgen (Figure 6B). Moreover, *HOTAIR* expression and androgen stimulation showed synergistic effects in maximizing AR binding.

To determine how these genomic binding events relate to target gene expression, we performed expression microarrays of hormone-deprived LNCaP cells with or without *HOTAIR* overexpression. To investigate how *HOTAIR* modulates the expression of androgen-regulated genes, we carried out gene set enrichment analysis (GSEA). Androgen-induced and -repressed gene sets were obtained from our previously published data in LNCaP cells stimulated with control or androgen (Zhao et al., 2012). Importantly, GSEA demonstrated that androgen-induced genes were significantly enriched for upregulation by *HOTAIR*, whereas androgen-repressed genes were downregulated (Figures 6C and 6D). Moreover, qRT-PCR analysis confirmed that androgen-induced genes, such as *PSA* and

Author Manuscript Author Manuscript Author Manuscript Author Manuscript

KLK2, were significantly increased, while androgen-repressed genes, including *NOV* and *OPRK1*, decreased following *HOTAIR* overexpression (Figures 6E and 6F).

To further characterize *HOTAIR* downstream genes, we carried out triplicate microarray experiments and identified 512 and 560 genes, respectively, that were significantly ($p < 0.01$) induced and repressed by *HOTAIR* in hormone-deprived LNCaP cells. To obtain some understanding of the function of these genes, we conducted gene ontology (GO) analysis and found that *HOTAIR*-induced genes were strongly enriched for cellular processes such as cell cycle, mitosis, and nuclear division (Table S2). *HOTAIR*-repressed genes, on the other hand, were involved in DNA binding, nucleus, and zinc-finger proteins (Table S3). Next, to determine how *HOTAIR* correlates with androgen signaling, we performed clustering analysis of triplicate microarray experiments profiling control and *HOTAIR*-overexpressing LNCaP cells before and after androgen stimulation. A heatmap analysis using Treeview demonstrated that a majority of *HOTAIR*-increased genes also were induced by androgen while *HOTAIR*-decreased genes were inhibited by androgen (Figure 6G). Moreover, these genes exhibited maximal regulation in LNCaP cells with *HOTAIR* overexpression and androgen stimulation.

To further confirm our findings, we treated control and *HOTAIR*-knockdown C4-2B with androgen and performed AR ChIP-seq. We observed that *HOTAIR* depletion decreased ARBSs in C4-2B cells under both androgen-deprived and -stimulated conditions. Interestingly, ARBSs found in androgen-stimulated, but *HOTAIR*-depleted, C4-2B cells largely overlapped with those found in androgen-deprived control cells, suggesting that *HOTAIR* knockdown counteracted the effect of androgen stimulation (Figure 6H). *HOTAIR* is required for AR-binding events in the milieu of low androgen, and *HOTAIR* collaborates with androgen in maximizing AR binding to chromatin (Figure 6I). Furthermore, ChIP-qPCR analysis confirmed that *HOTAIR* depletion abolished androgen-stimulated AR activation, while qRT-PCR assays validated that *HOTAIR* knockdown hampered AR transcriptional regulation (Figures 6J and 6K). Therefore, using two independent prostate cancer models, we demonstrated that *HOTAIR* overexpression induces an AR transcriptional program similar to that activated by androgen.

HOTAIR Promotes CRPC Progression

As androgen-independent AR activation is a main driver to CRPC, we next investigated the roles of *HOTAIR* in CRPC progression. Cell proliferation assays showed that *HOTAIR* overexpression significantly increased LNCaP cell growth, while *HOTAIR* knockdown in C4-2B cells markedly reduced cell growth, being consistent with its role in enhancing the AR transcriptional program (Figure 7A). As *HOTAIR* is able to drive androgen-independent AR activation, we performed cell proliferation assays in hormone-deprived PCa cells. Our results demonstrated that *HOTAIR* overexpression indeed increased LNCaP cell growth in the absence of androgen, whereas *HOTAIR* knockdown abolished androgen-independent C4-2B cell growth (Figure 7B). Besides cell growth, androgen signaling also is known to induce cell invasion. Boyden chamber assay showed that ectopic *HOTAIR* overexpression substantially increased LNCaP cell invasion (Figures 7C and 7D). On the other hand, *HOTAIR* depletion in C4-2B cells dramatically reduced cell invasion (Figures 7E and 7F).

Author Manuscript Author Manuscript Author Manuscript Author Manuscript

Therefore, being consistent with its role in enhancing AR chromatin-targeting and transcriptional activities, *HOTAIR* increases PCa cell growth and invasion.

Next, we attempted to investigate the role of *HOTAIR* in resistance to androgen-deprivation therapies. We generated enzalutamide-resistant cells by culturing LNCaP cells in the presence of 1 μM MDV3100 for several months. Our qRT-PCR analysis confirmed that *PSA* level was drastically decreased by MDV3100 initially and slowly recovered after 2 months of continuous drug treatment (Figure 7G). Interestingly, *HOTAIR* expression was gradually increased over time following the MDV3100 treatment and markedly upregulated to as much as 14-fold. Together with the role of *HOTAIR* in enhancing the androgen-independent AR program, these data suggest that *HOTAIR* upregulation may account at least partially for enzalutamide resistance and that *HOTAIR* knockdown may inhibit CRPC cell proliferation. Indeed, cell growth assays showed that *HOTAIR* knockdown further decreased C4-2B cell growth in the presence of enzalutamide (Figure 7H).

DISCUSSION

LncRNAs have been shown to regulate gene transcription and protein function through various mechanisms. For example, by binding to the PRC2 proteins, *HOTAIR* acts to guide and recruit PRC2 to target genes related with tumor metastasis in breast cancer (Gupta et al., 2010b). *HOTAIR* also can function as a scaffold that, by simultaneously binding to the EZH2 and LSD1 proteins through its 5′ end and 3′ end, respectively, direct these proteins to co-occupy the same genomic regions (Tsai et al., 2010). Through this scaffold function, *HOTAIR* also has been reported to link E3 ubiquitin ligases with their substrates to accelerate proteolysis (Yoon et al., 2013). Findings from our study revealed a distinct mode of action of lncRNAs in gene regulation. Here we propose a working model wherein the lncRNA *HOTAIR* binds the NTD of the AR protein, which consequently blocks recruitment of the E3 ubiquitin ligase MDM2 that interacts with AR through the same domain. Through this competitive mechanism, *HOTAIR* expression inhibits AR ubiquitination, prevents AR protein degradation, and, thus, increases AR protein stability. Our study demonstrates that the lncRNA is able to mask a protein-interacting domain, thereby preventing co-regulator protein binding.

In this paper, we show that *HOTAIR* is an androgen-repressed lncRNA that enhances the AR-activated gene expression program by directly binding to AR to protect it from ubiquitin-mediated degradation. In the absence of androgen, *HOTAIR* overexpression induced an AR-binding profile that largely overlapped with that induced by androgen, probably due to a shared mechanism of action, as androgen-induced ligand binding is well known to stabilize the AR protein (Zhou et al., 1995). In addition, a study by Steven Balk's laboratory previously found that AR itself is an androgen-repressed gene that is upregulated in CRPC to drive aberrant AR activity (Cai et al., 2011). Unlike androgen-induced genes, the androgen-repressed genes, such as *AR*, are able to escape from AR-mediated repression in CRPC cells and, thus, remain upregulated. *HOTAIR* may become upregulated in CRPC cells through similar mechanisms and further stabilize AR and enhance its activity.

Author Manuscript Author Manuscript Author Manuscript Author Manuscript

Being highly consistent with its positive regulation of AR signaling, *HOTAIR* overexpression in androgen-dependent LNCaP cells was found to increase cell growth even in the absence of androgen. On the other hand, *HOTAIR* knockdown in CRPC cell line C4-2B markedly decreased cell proliferation, supporting that *HOTAIR* expression is required for CRPC cell growth. Importantly, our results demonstrated that *HOTAIR* is remarkably upregulated in enzalutamide-resistant PCa cells and its depletion decreased CRPC cell growth in the presence of enzalutamide. The lncRNA *HOTAIR* thus may be a biomarker of enzalutamide resistance and a promising target for therapeutic intervention in CRPC.

EXPERIMENTAL PROCEDURES

Patient Specimens

Specimens were collected by the Northwestern University Prostate Cancer Specialized Program of Research Excellence Tissue Core (SPORE). Tissue samples were collected in a de-identified manner with informed consent of the patients and prior Institutional Review Board approval.

Plasmids and Reagents

The *HOTAIR* gene was amplified by RT-PCR and then cloned into a lentiviral vector pCDH-MSCV-mcs-EF1-GFP-T2A-Pu (SBI) at EcoR1 and Not1 sites using the Cold Fusion kit (SBI). To generate *HOTAIR* overexpression stable cells, cells were transduced with control or *HOTAIR* overexpression lentivirus particles and selected with puromycin for 3 days. *HOTAIR* knockdown construct was created by inserting oligo (CCGGGAACGGGAGTACAGAGAGAATCTCGAGATTCTCTCTGTACTCCCGTTCTTTTTG) into the pLKO.1 vector. Lentiviral particles were generated by transfecting 293T cells with packaging vectors, psPAX2 and pMD2.g. All primers were designed using Primer 3 and synthesized by Integrated DNA Technologies (Table S4). The qRT-PCR was performed using Bullseye EvaGreen qPCR SYBR Green Mastermix (MIDSCI) on an Applied Biosystems StepOne Plus. A detailed list of other plasmids and reagents used in this study is provided in the Supplemental Experimental Procedures.

RNA Pull-Down Assay

Biotin-labeled *HOTAIR* probe and cell protein extract were incubated for 60 min before being incubated with streptavidin agarose beads (Invitrogen) at room temperature (RT) for 1 hr. After PBS wash, the retrieved protein was subjected to western blot analysis. For detecting direct binding of AR with *HOTAIR*, AR-NT recombinant protein was incubated with biotin-labeled RNA probe to proceed with the IP process.

RIP

Briefly, cells were resuspended in radio-immunoprecipitation assay (RIPA) buffer and incubated with 20 μl protein beads and 1 μg antibody complex overnight at 4°C. After incubation with RNase-free DNase I (Promega) at 37°C for 15 min and proteinase K at 45°C for 45 min, RNA samples were extracted with 1 ml Trizol and subjected to RT-PCR analysis.

Author Manuscript Author Manuscript Author Manuscript Author Manuscript

LncRNA ISH

ISH was used to detect *HOTAIR* in clinical specimens. Biotin-labeled anti-sense *HOTAIR* LNA probe/5Biosg/G+C+C+TTGCTCCCTT+G+CCTGCATTTCT+C+T+G was synthesized by EXIQON. ISH was performed on paraffin-embedded PCa tissue microarray. Detailed procedure is provided in the Supplemental Experimental Procedures.

Gene Expression, ChIP-Seq, and Data Analysis

Total RNAs were isolated using TRIzol reagent (Invitrogen). The integrity of the RNA was monitored using Bioanalyzer 2100. Microarray profiling was performed using HumanHT-12 v 4.0 Expression BeadChip (Illumina). Bead-level data were processed using GenomeStudio (Illumina), and the expression values were quantile-normalized using the limma package in Bioconductor (Ritchie et al., 2015). Differentially expressed genes were identified based on $p < 0.01$. GO term enrichment was analyzed using DAVID 6.7 (Huang da et al., 2009). Heatmap view of differentially expressed genes was created by Cluster and Java Treeview (de Hoon et al., 2004; Saldanha, 2004).

ChIP was carried out as previously described (Yu et al., 2010). ChIP DNA was prepared into libraries according to standard protocols using Bioo Scientific's DNA Sample Kit (514101). Libraries were sequenced using Illumina Hi-Seq platforms. Sequence reads were aligned to the Human Reference Genome (assembly hg19) using Burrows-Wheeler Alignment Tool (bwa) version 0.6.1 (Li and Durbin, 2009). Peak identification and overlapping were performed using the Hypergeometric Optimization of Motif Enrichment suite (Heinz et al., 2010). Heatmaps and intensity plots of peaks were generated by Perk script, R, and/or Java Treeview.

Supplementary Material

Refer to Web version on PubMed Central for supplementary material.

Acknowledgments

We thank Dr. Ximing J. Yang (Northwestern University) for assistance on RNA ISH and Dr. Nicholas Erho (GenomeDx Biosciences) for data mining. Tissue microarrays were provided by the Northwestern University prostate cancer SPORE (P50 CA090386). J.K. and Y.A.Y were supported by the NIH T32 CA080621 and T32 CA09560, respectively. This work was supported in part by the NIH R01CA172384 (to J.Y.), U.S. Department of Defense W81XWH-14-1-0023 (to J.Y.), and the Research Scholar Award RSG-12-085-01 (to J.Y.) from the American Cancer Society.

References

Cai C, He HH, Chen S, Coleman I, Wang H, Fang Z, Chen S, Nelson PS, Liu XS, Brown M, Balk SP. Androgen receptor gene expression in prostate cancer is directly suppressed by the androgen receptor through recruitment of lysine-specific demethylase 1. Cancer Cell. 2011; 20:457–471. [PubMed: 22014572]

Chiyomaru T, Yamamura S, Fukuhara S, Yoshino H, Kinoshita T, Majid S, Saini S, Chang I, Tanaka Y, Enokida H, et al. Genistein inhibits prostate cancer cell growth by targeting miR-34a and oncogenic *HOTAIR*. PLoS ONE. 2013; 8:e70372. [PubMed: 23936419]

Dimitrova N, Zamudio JR, Jong RM, Soukup D, Resnick R, Sarma K, Ward AJ, Raj A, Lee JT, Sharp PA, Jacks T. LincRNA-p21 activates p21 in cis to promote Polycomb target gene expression and to enforce the G1/S checkpoint. Mol Cell. 2014; 54:777–790. [PubMed: 24857549]

Author Manuscript Author Manuscript Author Manuscript Author Manuscript

Du Z, Fei T, Verhaak RG, Su Z, Zhang Y, Brown M, Chen Y, Liu XS. Integrative genomic analyses reveal clinically relevant long non-coding RNAs in human cancer. Nat Struct Mol Biol. 2013; 20:908–913. [PubMed: 23728290]

Grasso CS, Wu YM, Robinson DR, Cao X, Dhanasekaran SM, Khan AP, Quist MJ, Jing X, Lonigro RJ, Brenner JC, et al. The mutational landscape of lethal castration-resistant prostate cancer. Nature. 2012; 487:239–243. [PubMed: 22722839]

Gupta RA, Shah N, Wang KC, Kim J, Horlings HM, Wong DJ, Tsai MC, Hung T, Argani P, Rinn JL, et al. Long non-coding RNA *HOTAIR* reprograms chromatin state to promote cancer metastasis. Nature. 2010a; 464:1071–1076. [PubMed: 20393566]

Gupta S, Iljin K, Sara H, Mpindi JP, Mirtti T, Vainio P, Rantala J, Alanen K, Nees M, Kallioniemi O. FZD4 as a mediator of ERG oncogene-induced WNT signaling and epithelial-to-mesenchymal transition in human prostate cancer cells. Cancer Res. 2010b; 70:6735–6745. [PubMed: 20713528]

Heinz S, Benner C, Spann N, Bertolino E, et al. Simple Combinations of Lineage-Determining Transcription Factors Prime cis-Regulatory Elements Required for Macrophage and B Cell Identities. Mol Cell. 2010; 38(4):576–589. [PubMed: 20513432]

Hu X, Feng Y, Zhang D, Zhao SD, Hu Z, Greshock J, Zhang Y, Yang L, Zhong X, Wang LP, et al. A functional genomic approach identifies FAL1 as an oncogenic long noncoding RNA that associates with BMI1 and represses p21 expression in cancer. Cancer Cell. 2014; 26:344–357. [PubMed: 25203321]

Huang da W, Sherman BT, Lempicki RA. Systematic and integrative analysis of large gene lists using DAVID bioinformatics resources. Nat Protoc. 2009; 4:44–57. [PubMed: 19131956]

Iyer MK, Niknafs YS, Malik R, Singhal U, Sahu A, Hosono Y, Barrette TR, Prensner JR, Evans JR, Zhao S, et al. The landscape of long noncoding RNAs in the human transcriptome. Nat Genet. 2015; 47:199–208. [PubMed: 25599403]

Khalil AM, Guttman M, Huarte M, Garber M, Raj A, Rivea Morales D, Thomas K, Presser A, Bernstein BE, van Oudenaarden A, et al. Many human large intergenic noncoding RNAs associate with chromatin-modifying complexes and affect gene expression. Proc Natl Acad Sci USA. 2009; 106:11667–11672. [PubMed: 19571010]

Kim K, Jutooru I, Chadalapaka G, Johnson G, Frank J, Burghardt R, Kim S, Safe S. *HOTAIR* is a negative prognostic factor and exhibits pro-oncogenic activity in pancreatic cancer. Oncogene. 2013; 32:1616–1625. [PubMed: 22614017]

Kogo R, Shimamura T, Mimori K, Kawahara K, Imoto S, Sudo T, Tanaka F, Shibata K, Suzuki A, Komune S, et al. Long noncoding RNA *HOTAIR* regulates polycomb-dependent chromatin modification and is associated with poor prognosis in colorectal cancers. Cancer Res. 2011; 71:6320–6326. [PubMed: 21862635]

Li H, Durbin R. Fast and accurate short read alignment with Burrows-Wheeler Transform. Bioinformatics. 2009; 25:1754–1760. [PubMed: 19451168]

Lin HK, Wang L, Hu YC, Altuwaijri S, Chang C. Phosphorylation-dependent ubiquitylation and degradation of androgen receptor by Akt require Mdm2 E3 ligase. EMBO J. 2002; 21:4037–4048. [PubMed: 12145204]

de Hoon MJL, Imoto S, Nolan J, Miyano S. Open Source Clustering Software. Bioinformatics. 2004; 20(9):1453–1454. [PubMed: 14871861]

Nakagawa T, Endo H, Yokoyama M, Abe J, Tamai K, Tanaka N, Sato I, Takahashi S, Kondo T, Satoh K. Large noncoding RNA *HOTAIR* enhances aggressive biological behavior and is associated with short disease-free survival in human non-small cell lung cancer. Biochem Biophys Res Commun. 2013; 436:319–324. [PubMed: 23743197]

Prensner JR, Iyer MK, Balbin OA, Dhanasekaran SM, Cao Q, Brenner JC, Laxman B, Asangani IA, Grasso CS, Kominsky HD, et al. Transcriptome sequencing across a prostate cancer cohort identifies PCAT-1, an unannotated lincRNA implicated in disease progression. Nat Biotechnol. 2011; 29:742–749. [PubMed: 21804560]

Prensner JR, Iyer MK, Sahu A, Asangani IA, Cao Q, Patel L, Vergara IA, Davicioni E, Erho N, Ghadessi M, et al. The long noncoding RNA SChLAP1 promotes aggressive prostate cancer and antagonizes the SWI/SNF complex. Nat Genet. 2013; 45:1392–1398. [PubMed: 24076601]

Author Manuscript Author Manuscript Author Manuscript Author Manuscript

Prensner JR, Sahu A, Iyer MK, Malik R, Chandler B, Asangani IA, Poliakov A, Vergara IA, Alshalalfa M, Jenkins RB, et al. The IncRNAs PCGEM1 and PRNCR1 are not implicated in castration resistant prostate cancer. Oncotarget. 2014; 5:1434–1438. [PubMed: 24727738]

Rinn JL, Chang HY. Genome regulation by long noncoding RNAs. Annu Rev Biochem. 2012; 81:145–166. [PubMed: 22663078]

Ritchie ME, Phipson B, Wu D, Hu Y, Law CW, Shi W, Smyth GK. Limma powers differential expression analyses for RNA-sequencing and microarray studies. Nucleic Acids Research. 2015; 43(7)

Saldanha AJ. Java Treeview-extensible visualization of microarray data. Bioinformatics. 2004; 20(17): 3246–3248. [PubMed: 15180930]

Sørensen KP, Thomassen M, Tan Q, Bak M, Cold S, Burton M, Larsen MJ, Kruse TA. Long non-coding RNA *HOTAIR* is an independent prognostic marker of metastasis in estrogen receptor-positive primary breast cancer. Breast Cancer Res Treat. 2013; 142:529–536. [PubMed: 24258260]

Tsai MC, Manor O, Wan Y, Mosammaparast N, Wang JK, Lan F, Shi Y, Segal E, Chang HY. Long noncoding RNA as modular scaffold of histone modification complexes. Science. 2010; 329:689–693. [PubMed: 20616235]

Yang L, Lin C, Jin C, Yang JC, Tanasa B, Li W, Merkurjev D, Ohgi KA, Meng D, Zhang J, et al. lncRNA-dependent mechanisms of androgen-receptor-regulated gene activation programs. Nature. 2013; 500:598–602. [PubMed: 23945587]

Yoon JH, Abdelmohsen K, Kim J, Yang X, Martindale JL, Tominaga-Yamanaka K, White EJ, Orjalo AV, Rinn JL, Kreft SG, et al. Scaffold function of long non-coding RNA *HOTAIR* in protein ubiquitination. Nat Commun. 2013; 4:2939. [PubMed: 24326307]

Yu J, Yu J, Mani RS, Cao Q, Brenner CJ, Cao X, Wang X, Wu L, Li J, Hu M, et al. An integrated network of androgen receptor, polycomb, and TMPRSS2-ERG gene fusions in prostate cancer progression. Cancer Cell. 2010; 17:443–454. [PubMed: 20478527]

Zhao JC, Yu J, Runkle C, Wu L, Hu M, Wu D, Liu JS, Wang Q, Qin ZS, Yu J. Cooperation between Polycomb and androgen receptor during oncogenic transformation. Genome Res. 2012; 22:322–331. [PubMed: 22179855]

Zhou ZX, Lane MV, Kemppainen JA, French FS, Wilson EM. Specificity of ligand-dependent androgen receptor stabilization: receptor domain interactions influence ligand dissociation and receptor stability. Mol Endocrinol. 1995; 9:208–218. [PubMed: 7776971]

Author Manuscript Author Manuscript Author Manuscript Author Manuscript

Highlights

- The lncRNA *HOTAIR* is repressed by androgen and, thus, upregulated in CRPC
- *HOTAIR* inhibits AR degradation by blocking its binding to E3 ubiquitin ligase MDM2
- *HOTAIR* increases AR chromatin targeting and enhances the AR-mediated gene program
- *HOTAIR* drives androgen-independent AR activation and promotes CRPC

Author Manuscript Author Manuscript Author Manuscript Author Manuscript

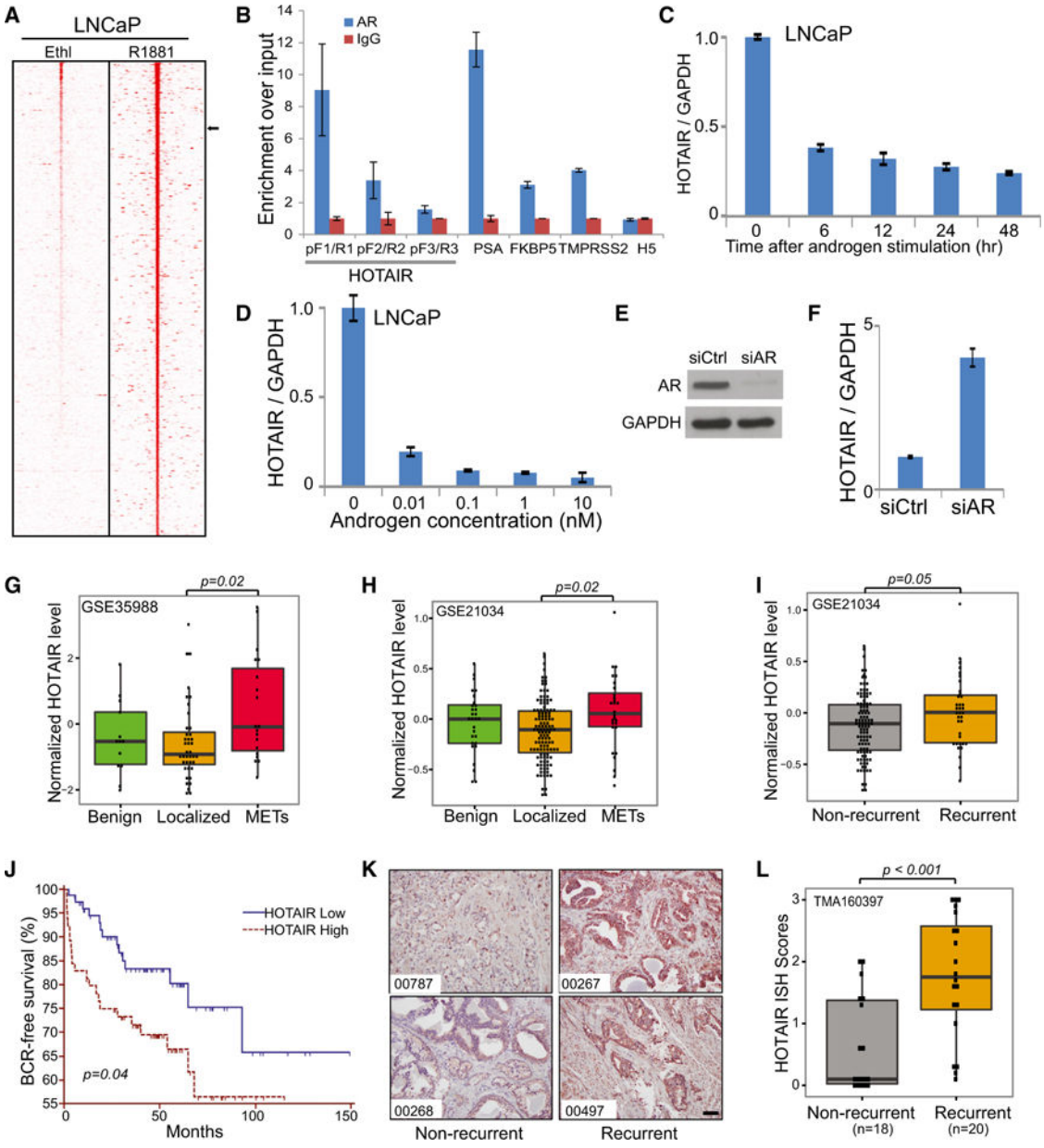

Figure 1. *HOTAIR* Is Repressed by Androgen and Is Thus Upregulated in CRPC

(A) Heatmap showing AR ChIP-seq reads around lncRNAs. Previously published AR ChIP-seq data from ethanol or R1881 (10 nM)-stimulated LNCaP cells were re-analyzed for enrichment around lncRNAs (Table S1). Normalized AR ChIP-seq reads around (±50 kb) lncRNAs are shown. Black arrow on the right denotes *HOTAIR*.

(B) AR occupies the *HOTAIR* promoter. AR and IgG ChIP were performed in LNCaP cells and ChIP-qPCR was carried out using primers flanking the *HOTAIR* promoter regions (see Figure S1B for detail), well-established AR target gene enhancers, and the 3′ end of the *HOTAIR* gene as a negative control (H5).

(C and D) Androgen inhibits *HOTAIR* expression. The qRT-PCR analysis of *HOTAIR* expression in LNCaP cells, stimulated either by 1 nM androgen R1881 over a time course

Author Manuscript Author Manuscript Author Manuscript Author Manuscript

(C) or by different doses of R1881 (D) for 48 hr, is shown. Data were normalized to *GAPDH*. Data shown are mean ± SEM and representative of at least two independent experiments.

(E and F) AR depletion restores *HOTAIR* expression. LNCaP cells were treated with control and AR-targeting small interfering RNA (siRNA), confirmed for AR knockdown (E) and subjected to qRT-PCR analysis of *HOTAIR* expression (F).

(G–I) *HOTAIR* is upregulated in metastatic prostate tumors. *HOTAIR* expression in publicly available datasets (GEO: GSE35988 and GSE21034) was comparatively plotted in benign prostate, localized PCa, and metastatic PCa (G and H) or in localized PCa with or without biochemical recurrence (I). Significant p values are indicated.

(J) High *HOTAIR* level is associated with poor clinical outcome. Kaplan-Meier analysis of PCa outcome using the GEO: GSE21034 dataset is shown. Localized PCa cases were stratified based on their *HOTAIR* expression level and analyzed for biochemical recurrence. The p values for Kaplan-Meier curves were determined using a log-rank test.

(K and L) The lncRNA ISH was performed using a tissue microarray of recurrent versus non-recurrent PCa. ISH *HOTAIR* staining in two representative cases of recurrent and non-recurrent PCa is shown (K). Scale bar, 100 μm. *HOTAIR* ISH staining intensity was scored in all cases, compared between two groups ($p < 0.001$ by t test), and visualized by boxplot (L).

Author Manuscript Author Manuscript Author Manuscript Author Manuscript

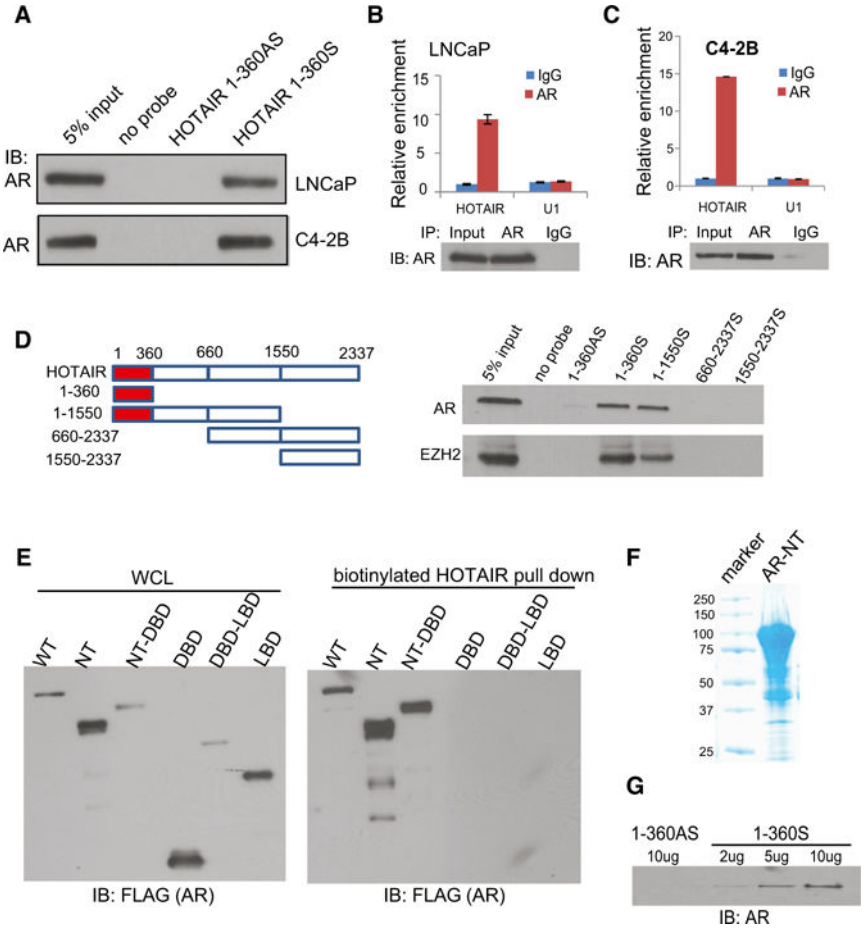

Figure 2. *HOTAIR* Directly Interacts with the AR Protein

(A) Western blot showing AR protein interaction with *HOTAIR* RNA. RNA pull-down assay was performed in LNCaP and C4-2B cells using biotin-labeled *HOTAIR* RNA probe transcribed in vitro from the first 360 bp of the sense *HOTAIR* gene and detected using western blots. No probe and *HOTAIR* 1–360AS probe were used as negative controls.

(B and C) The qRT-PCR showing *HOTAIR* enrichment by an anti-AR antibody. LNCaP (B) and C4-2B (C) cells were subjected to RIP assay using an anti-AR antibody or IgG. IP-enriched RNA was then analyzed by qRT-PCR using U1 RNA as a negative control. (Bottom) Western blots confirm AR protein IP. Error bars are mean ± SEM.

(D) The 5′ end of *HOTAIR* transcript binds AR. RNA pull-down was carried out in LNCaP cells with various *HOTAIR* deletion probes (top), and the retrieved protein extract was analyzed by western blotting (bottom).

(E) NTD of the AR protein interacts with *HOTAIR*. FLAG-tagged AR deletion constructs were transfected into 293T cells and the expression confirmed by western blot analysis (left). RNA pull-down using biotinylated *HOTAIR* 1–360S probe retrieved the NTD-containing AR proteins (right).

(F and G) Coomassie blue staining verifying purified recombinant MBP-AR-NT protein synthesized in vitro (F) and western blot of AR-NT proteins retrieved by increasing doses of *HOTAIR* probes in in vitro binding assay (G). *HOTAIR* 1–360AS probe was used as a negative control.

Author Manuscript Author Manuscript Author Manuscript Author Manuscript

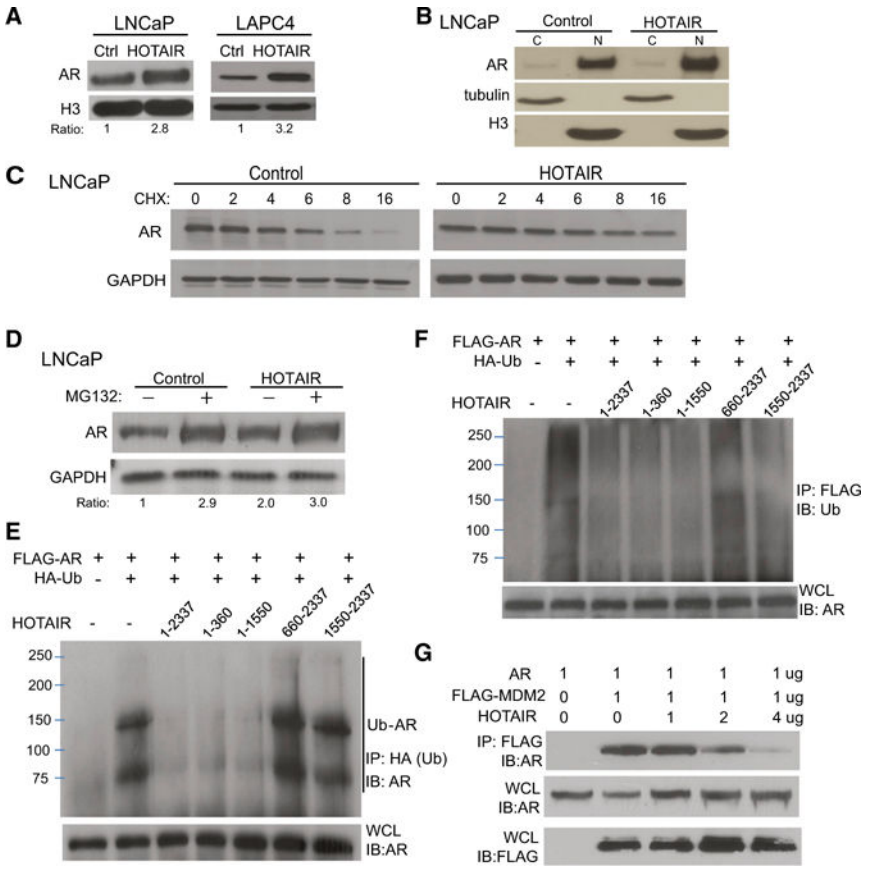

Figure 3. *HOTAIR* Stabilizes AR and Blocks MDM2-Mediated Ubiquitination

(A) Western blot shows total AR protein level in control and *HOTAIR*-overexpressing LNCaP and LAPC4 cells.

(B) Cytoplasmic and nuclear AR protein levels in control and *HOTAIR*-overexpressing LNCaP cells. Tubulin and H3 were used as cytoplasmic and nuclear protein-loading controls, respectively.

(C) *HOTAIR* overexpression stabilizes AR protein. Control, *HOTAIR*-overexpressing LNCaP cells were treated with 10 μM CHX for 6 hr and then collected at the indicated times for western blotting.

(D) Effects of proteasome inhibitor MG132 on *HOTAIR*-mediated AR protein level. LNCaP cells with control or *HOTAIR* overexpression were treated with control or 10 μM MG132 for 6 hr and subjected to western blot analysis.

(E and F) *HOTAIR* regulation of AR ubiquitination. The FLAG-AR and HA-Ub constructs were co-transfected into 293T cells with different regions of the *HOTAIR* transcript. (E) Whole-cell lysates (WCLs) were confirmed for AR expression (bottom) and subjected to IP using an anti-HA (Ub) antibody, followed by western blot using an anti-AR antibody (top). In a reverse coIP (F), WCLs were subjected to IP using an anti-FLAG (AR) antibody, followed by western blot using an anti-Ubiquitin antibody.

(G) CoIP showing AR and MDM2 protein interaction. The 293T cells were co-transfected with AR and different amounts of FLAG-MDM2 and *HOTAIR*. Cell lysates were confirmed for the expression of AR and MDM2 using anti-AR and anti-FLAG (MDM2) antibodies,

Author Manuscript Author Manuscript Author Manuscript Author Manuscript

respectively. CoIP using anti-FLAG (MDM2) followed by anti-AR western blot detected a reduced amount of AR pulled down following *HOTAIR* overexpression.

Author Manuscript Author Manuscript Author Manuscript Author Manuscript

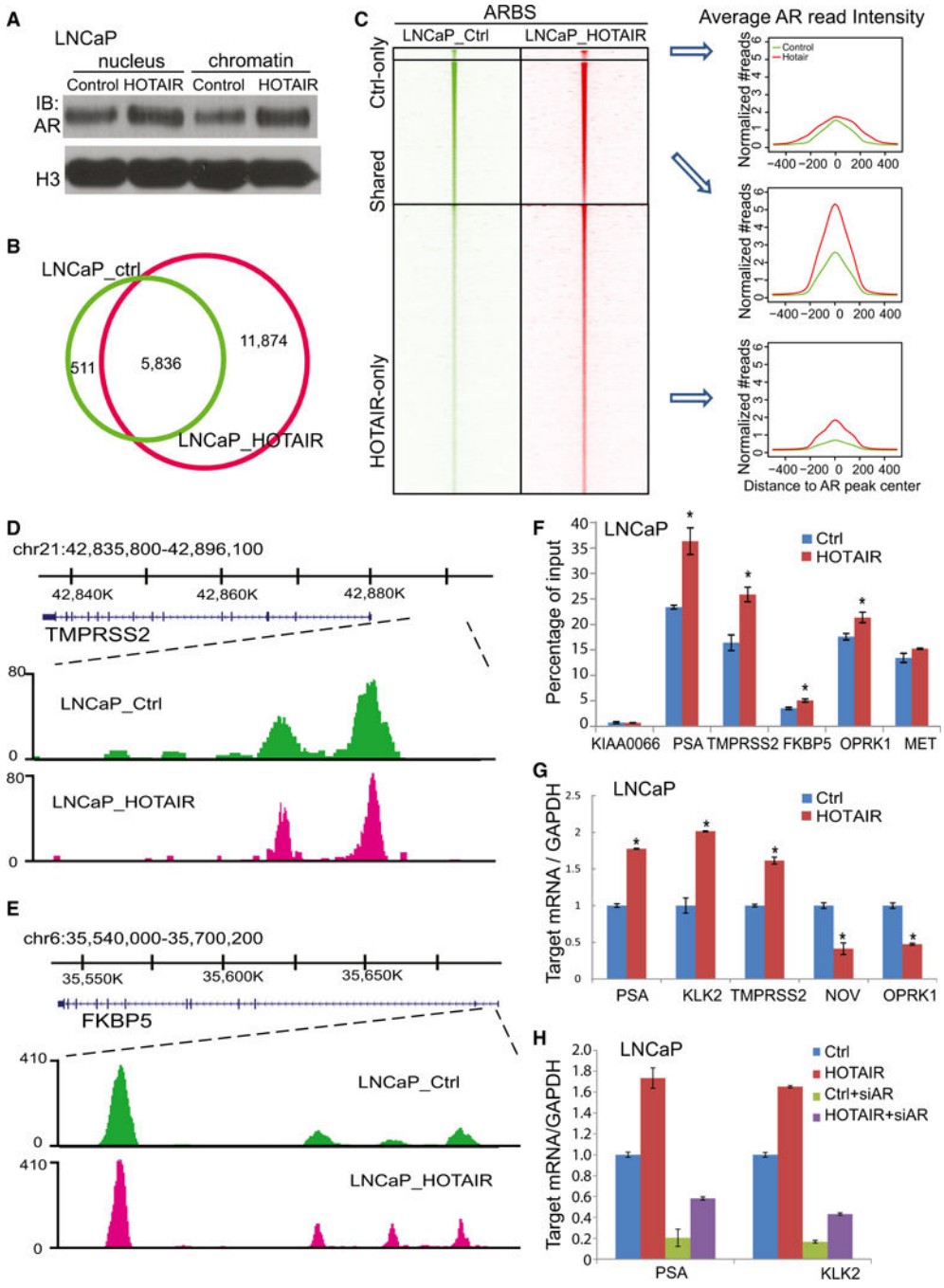

Figure 4. *HOTAIR* Expression Enhances AR Transcriptional Activity

(A) Nuclear and chromatin-bound fractions of AR protein in control and *HOTAIR*-overexpressing LNCaP cells. H3 was used as a loading control.

(B) Overlap of AR-binding sites (ARBSs) detected by ChIP-seq in LNCaP cells with control (LNCaP_ctrl) or *HOTAIR* overexpression (LNCaP_*HOTAIR*) is shown.

(C) Heatmap depicting AR ChIP-seq read intensity around (±5 kb) ARBSs detected in control only, *HOTAIR*-overexpressing LNCaP cells only, or both. Average AR ChIP-seq read intensity around ARBSs (±500 bp) is shown (right).

Author Manuscript Author Manuscript Author Manuscript Author Manuscript

(D and E) Genome browser view of ChIP-seq AR-binding events around known AR downstream genes *TMPRSS2* (D) and *FKBP5* (E) is shown.

(F) ChIP-qPCR analysis of known AR target genes. AR ChIP was performed in LNCaP_ctrl and LNCaP_*HOTAIR* cells followed by qPCR using primers targeting enhancers of several AR downstream genes. *KIAA0066* was used as a negative control. Data shown are mean ± SEM.

(G) The qRT-PCR analysis of AR downstream genes in LNCaP cells with control, *HOTAIR* overexpression. Gene expression was normalized to *GAPDH*. Data shown are mean ± SEM.

(H) The qRT-PCR analysis of AR downstream genes in LNCaP_ctrl and LNCaP_*HOTAIR* cells with control or AR knockdown. Gene expression was normalized to *GAPDH*. Data shown are mean ± SEM.

Author Manuscript Author Manuscript Author Manuscript Author Manuscript

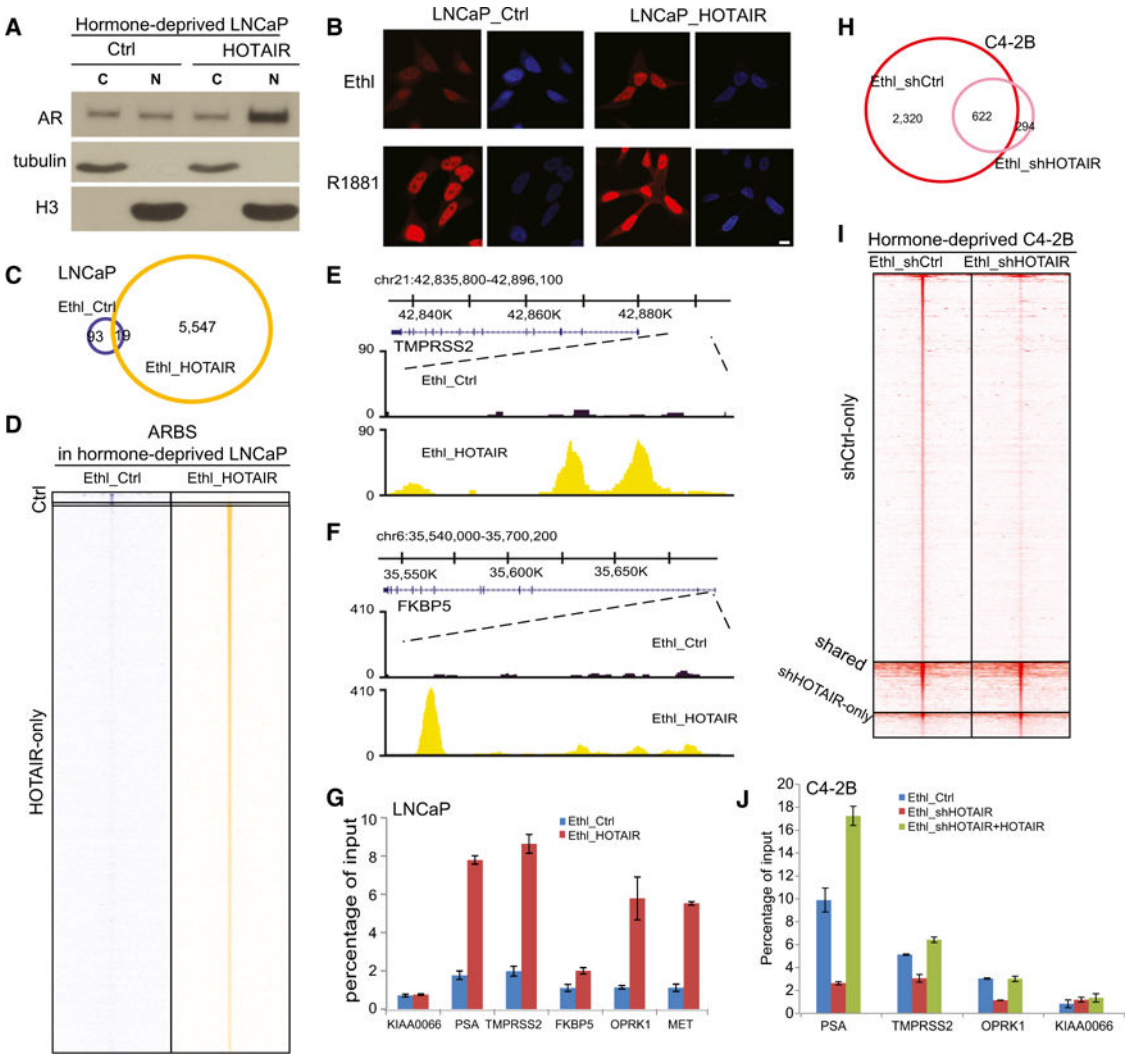

Figure 5. *HOTAIR* Overexpression Leads to Androgen-Independent AR Chromatin Targeting

(A) Cytoplasmic and nuclear AR protein levels in hormone-deprived, control and *HOTAIR*-overexpressing LNCaP cells. Tubulin and H3 were used as cytoplasmic and nuclear protein-loading controls, respectively.

(B) Immunofluorescence staining of AR. LNCaP_ctrl and LNCaP_*HOTAIR* cells were hormone-starved for 3 days and treated with ethanol or 1 nM R1881 for 24 hr before being subjected to immunostaining using an anti-AR antibody. Scale bar, 10 μm.

(C) Overlap of ARBSs detected in hormone-deprived LNCaP_ctrl and LNCaP_*HOTAIR* cells is shown.

(D) Heatmap depicts AR ChIP-seq read intensity around (±5 kb) ARBSs shown in (C).

(E and F) Genome browser view of ChIP-seq AR-binding events around AR target genes *TMPRSS2* (E) and *FKBP5* (F) is shown.

(G) ChIP-qPCR of AR binding on known target genes. AR ChIP was performed in hormone-deprived LNCaP_ctrl and LNCaP_*HOTAIR* cells. *KIAA0066* was the negative control gene. Data shown are mean ± SEM.

Author Manuscript Author Manuscript Author Manuscript Author Manuscript

(H) Overlap of ARBSs detected in C4-2B cells with control or *HOTAIR* knockdown is shown.

(I) Heatmap depicts AR ChIP-seq read intensity around (±5 kb) ARBSs shown in (H).

(J) ChIP-qPCR of AR binding on known target genes. AR ChIP was performed in hormone-deprived C4-2B_ctrl, C4-2B sh*HOTAIR*, and C4-2B sh*HOTAIR* + *HOTAIR* WT cells. *KIAA0066* was the negative control gene. Data shown are mean ± SEM.

Author Manuscript Author Manuscript Author Manuscript Author Manuscript

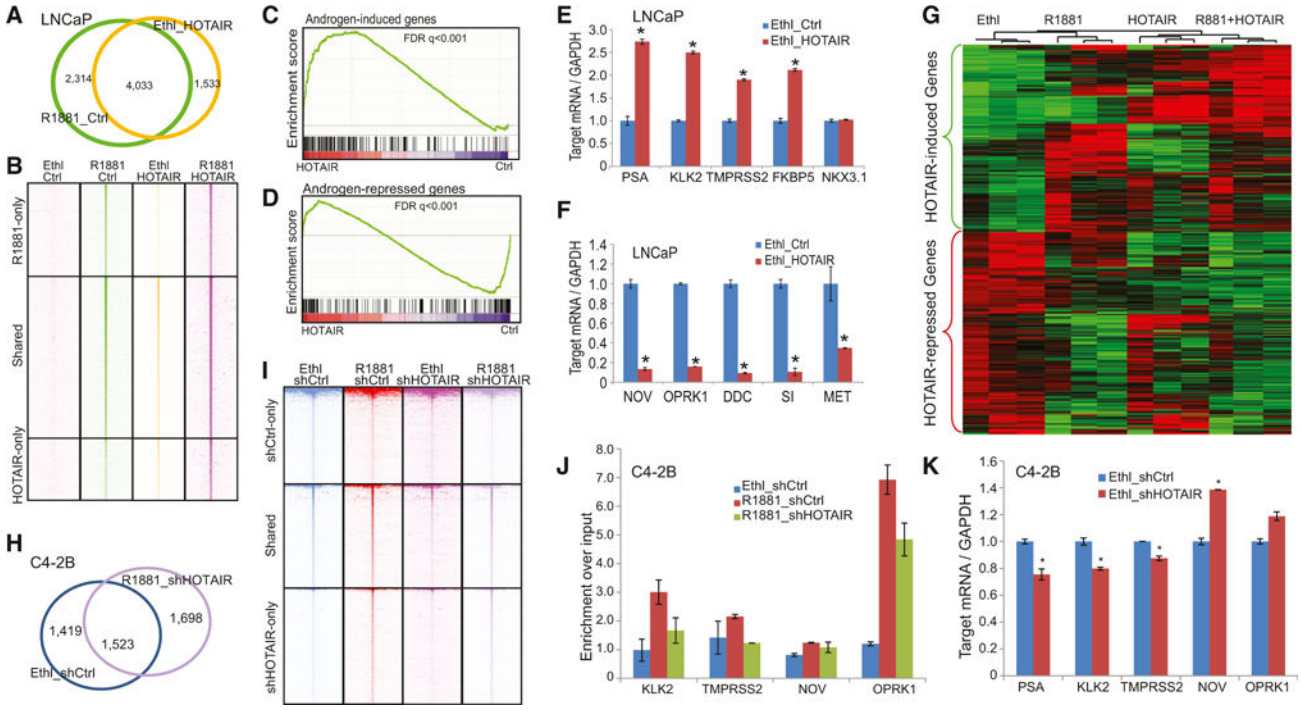

Figure 6. *HOTAIR* Drives AR Transcriptional Program in the Absence of Androgen

(A) Overlap of ARBSs detected in hormone-deprived LNCaP cells with either R1881 or *HOTAIR* overexpression is shown.

(B) Heatmap depicting AR ChIP-seq read intensity around (±5 kb) ARBSs shown in (A). AR ChIP-seq was carried out in LNCaP cells treated with R1881, *HOTAIR* overexpression, or both. ChIP-seq enrichment was normalized to total number of reads for comparative visualization.

(C and D) GSEA depicting *HOTAIR* regulation of AR-mediated gene program. GSEA was carried out to determine the enrichment of AR-induced (C) and AR-repressed (D) gene sets in expression dataset profiling hormone-deprived LNCaP cells with control or *HOTAIR* overexpression.

(E and F) The qRT-PCR analysis of AR-induced (E) and AR-repressed (F) genes in hormone-deprived LNCaP with control or *HOTAIR* overexpression. Data were normalized to *GAPDH*. Error bars are mean ± SEM.

(G) Heatmap view of *HOTAIR*-regulated genes in triplicate microarray experiments profiling hormone-deprived LNCaP_ctrl and LNCaP_*HOTAIR* cells stimulated with ethanol or androgen. Each row represents one gene, and each column corresponds to one expression microarray. Differentially expressed genes were identified by limma R package with p value cutoff <0.01.

(H) Overlap of ARBSs detected in C4-2B cells with hormone-deprivation or *HOTAIR* knockdown is shown.

(I) Heatmap depicting AR ChIP-seq read intensity around (±5 kb) ARBSs shown in (H). AR ChIP-seq was carried out in C4-2B cells treated with R1881, *HOTAIR* knockdown, or both. ChIP-seq enrichment was normalized to the total number of reads for comparative visualization.

Author Manuscript Author Manuscript Author Manuscript Author Manuscript

(J) AR ChIP was performed in C4-2B_shCtrl or C4-2B-sh*HOTAIR* cells in the presence or absence of androgen. ChIP-qPCR was carried out using primers targeting enhancers of different AR downstream genes. *KIAA0066* was the negative control. Error bars are mean ± SEM.

(K) The qRT-PCR analysis of AR downstream genes in C4-2B_shCtrl and C4-2B-sh*HOTAIR* cells cultured in hormone starvation medium. Data were normalized to *GAPDH*. Error bars are mean ± SEM.

Author Manuscript Author Manuscript Author Manuscript Author Manuscript

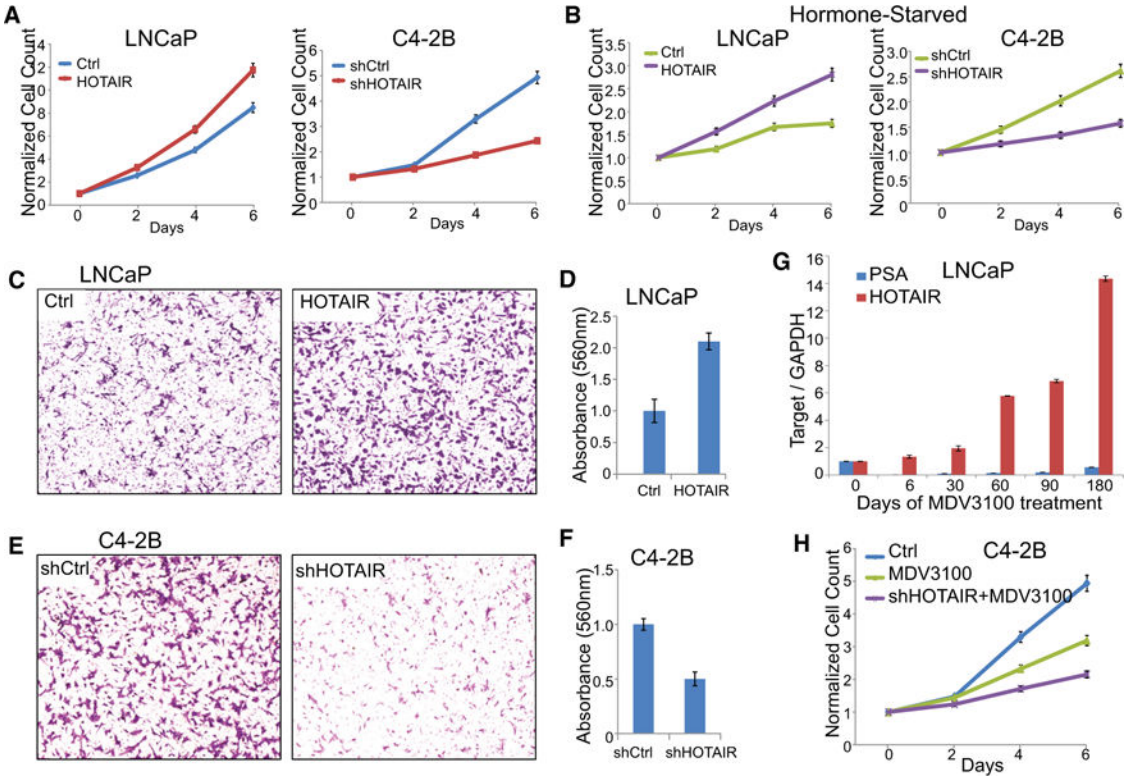

Figure 7. *HOTAIR* Promotes CRPC Progression

(A) *HOTAIR* regulation of androgen-dependent cell growth. Cell growth was assayed in LNCaP cells with control or *HOTAIR* overexpression and C4-2B cells with control or *HOTAIR* knockdown. Cells were grown in androgen-containing medium. Data shown are mean ± SEM of triplicate wells and are representative of at least two replicate experiments.

(B) *HOTAIR* regulation of androgen-independent growth of LNCaP and C4-2B cells grown in hormone-deprived condition is shown.

(C and D) *HOTAIR* overexpression increases LNCaP cell invasion. Cell invasion was monitored by Boyden chamber assay in LNCaP_Ctrl and LNCaP_*HOTAIR* cells. Representative images of invaded cells are shown (C), and the total number of invaded cells was quantified using colorimetry with absorbance at 560 nm (D). (E and F) *HOTAIR* depletion diminished C4-2B cell invasion as examined using Boyden chamber assay. Representative images of invaded cells are shown (E), and the total number of invaded cells was quantified using colorimetry with absorbance at 560 nm (F).

(G) The qRT-PCR showing PSA and *HOTAIR* expression in LNCaP cells following MDV3100 treatment. Gene expression was normalized to *GAPDH*. Error bars are mean ± SEM.

(H) Cell growth of C4-2B cells treated with MDV3100 alone or in combination with *HOTAIR* depletion is shown.